Electroless composite coating of Ni–P–carbon nanotubes on magnesium powder

Mahan Firoozbakht, Sayed Mahmoud Monirvaghefi, Behzad Niroumand *

Department of Materials Engineering, Isfahan University of Technology, Isfahan 84156-83111, Iran

ABSTRACT

The high tendency of carbon nanotubes (CNTs) for agglomeration makes their uniform dispersion as reinforcement in bulk metal matrix composites a great challenge. A promising new way is introduced in this paper whereby CNTs are uniformly deposited on metallic particles which can be used later for production of CNT reinforced bulk metal matrix composites. In this study, for the first time, composite coatings of Ni–P–CNT were successfully co-deposited on magnesium powder through electroless plating method. Effects of such processing parameters as pH, temperature and CNT content were studied and suitable coating conditions were identified. The results showed a good distribution of individual CNTs in the composite coating and minimal coating separation produced under suitable electroless coating conditions. The Ni–P–CNT coated magnesium powder could be used as the feedstock for production of bulk magnesium nano-composites.

1. Introduction

Carbon nanotube (CNT) has recently emerged as a one-dimensional nano-material [1] with a unique chemical structure [1–3] and exceptional mechanical, thermal and electrical properties exceeding those of any conventional material [4–8]. The distinctive mechanical properties of CNT, such as its extraordinary high strength and toughness, make it an ideal candidate as reinforcement in metal matrix composites to improve mechanical properties while also contributing to weight saving [5–9]. However, due to the attractive Van der Waals interactions, CNTs tend to form aggregates which make their dispersion in the matrix and obtaining a good distribution of the reinforcements a big challenge [5,8,10,11]. Moreover, due to poor wettability of CNTs by molten metals, segregation occurs during liquid metal composite processing [11,12], and because of weak bonding between the matrix and the reinforcements, load transfer from the matrix to the reinforcements will be low [5,11,13]. Therefore, these problems should be addressed before CNT can be used as reinforcement in bulk metal matrix nano-composites.

To surmount these obstacles, such ways as coating the CNTs, or putting them in a coating, has been suggested [11–13]. By placing CNTs into a metal coating, i.e., making a composite coating, such advantages as similarity of the surface energy to that of the matrix metal can be obtained.

One way of producing composite coatings is co-deposition of particles into a metal matrix from an electroless bath [3–5,14–16].

Nickel–phosphorous is one of the most popular electroless coatings in this regard, and because of its good wear properties, corrosion resistance, uniform coating thickness and applicability for a variety of materials and surfaces [1,14,17].

Electroless nickel deposition can be viewed as the sum of two chemical reactions, i.e., a chemical oxidation reaction that liberates electrons and a nickel reduction reaction that consumes electrons [18]. Nickel sulphate and sodium hypophosphite have been widely used in electroless Ni–P coatings as the preferred source of nickel cations and the reducing agent, respectively [18]. Electroless nickel plating process can be divided into the following basic steps: diffusion and absorption of the reactants (Ni^{2+} and $H_2PO_2^-$) to the surface, chemical reaction on the surface and desorption of the products (HPO_3^-, H_2 and H^+) [18]. The reaction is a function of temperature and pH of the electroless bath. It has been shown that the rate of reduction and oxidation reactions will level up by increasing the temperature. Also a concurrent increase in the deposition rate is the most noticeable change in the plating process when pH increases [18].

It has been recognized that, under suitable coating conditions and reasonable coating growth rates, the growing layer can entangle the particles in its vicinity and results in formation of composite coatings [18]. Depending on the particles nature, incorporation of particles into a Ni–P matrix provides enhanced surface properties [14–17].

With the development of modern science, micrometer composite coatings could not more fully meet the needs of critical applications. Electroless nano-composite coatings, in which nanoparticles are used as the reinforcement, are therefore considered nowadays for such applications owing to their excellent performances [1,3,6,15].

* Corresponding author. Tel.: +98 311 3915731; fax: +98 311 3912752.
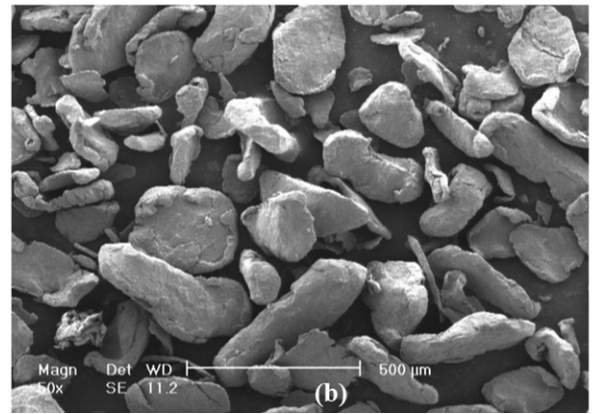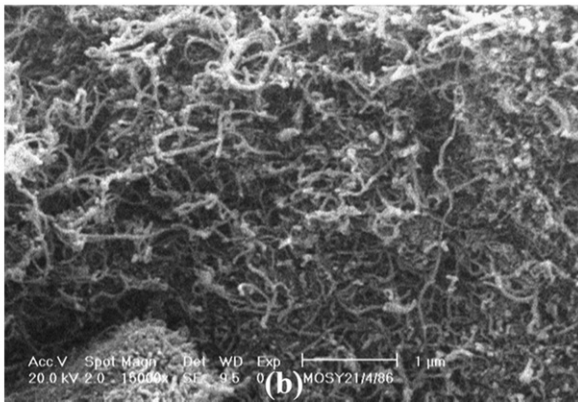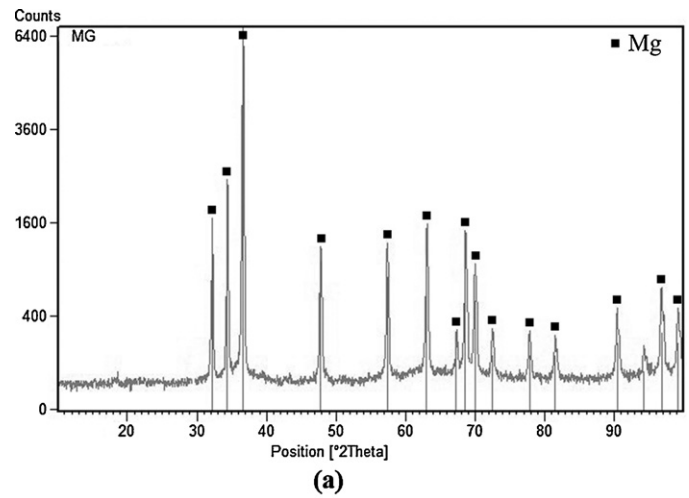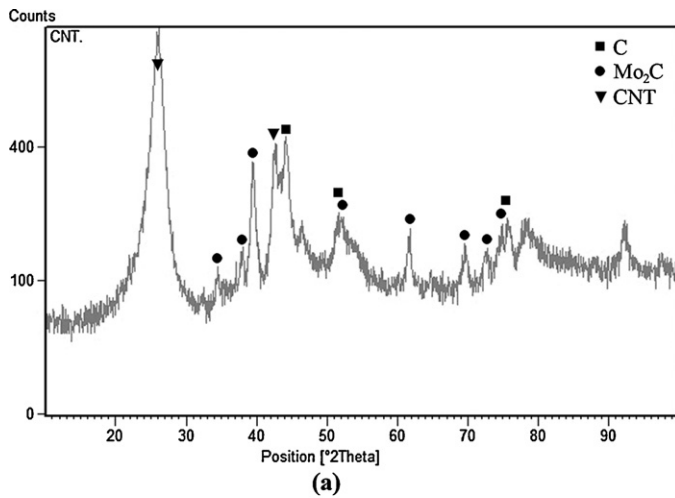 E-mail address: behzn@cc.iut.ac.ir (B. Niroumand).

Fig. 1. (a) XRD pattern of CNTs and (b) SEM image of CNT agglomerates.

Fig. 2. (a) XRD pattern and (b) SEM image of magnesium powder.

Several published reports on the introduction of CNTs to Ni–P electroless coatings [4–7] show that the co-deposited CNTs greatly increase the tribological properties of the coating. It has been also reported that, under suitable coating conditions, CNT agglomeration problem can be overcome by electroless coating process and a uniform CNT dispersion in the nickel matrix can be realized [2,7]. However, achieving a uniform CNT distribution in the coating requires provision of homogeneous suspension of CNTs in the electroless bath [5].

Studying the literature on electroless composite coating reveals that all the electroless coatings so far have been applied on the bulk stationary surfaces in the electroless bath. One exception is the work of two of the present authors on electroless Ni–P–CNT coating on aluminum powder [19]. In this paper we describe our successful attempt to achieve a uniform composite coating of Ni–P–CNT on magnesium powder with minimal CNT agglomeration in the composite coatings.
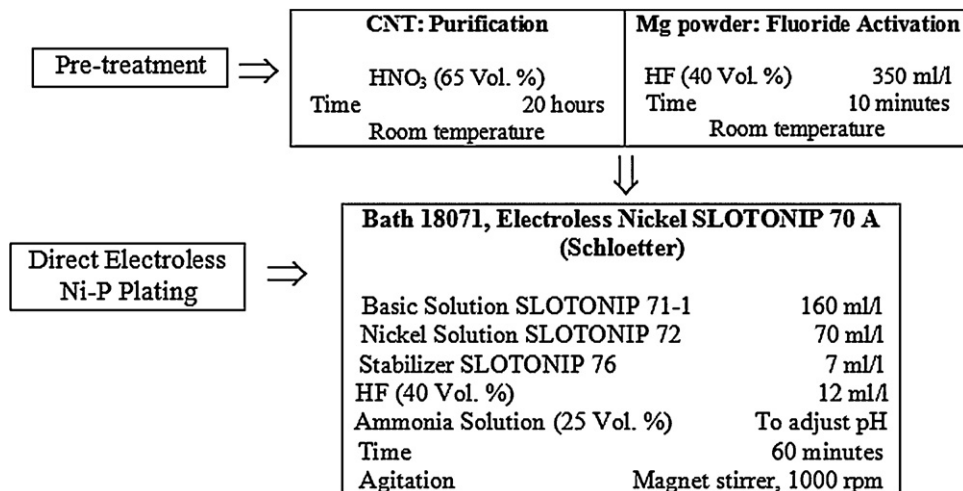

Fig. 3. Different stages of electroless coating process and the coating parameters.
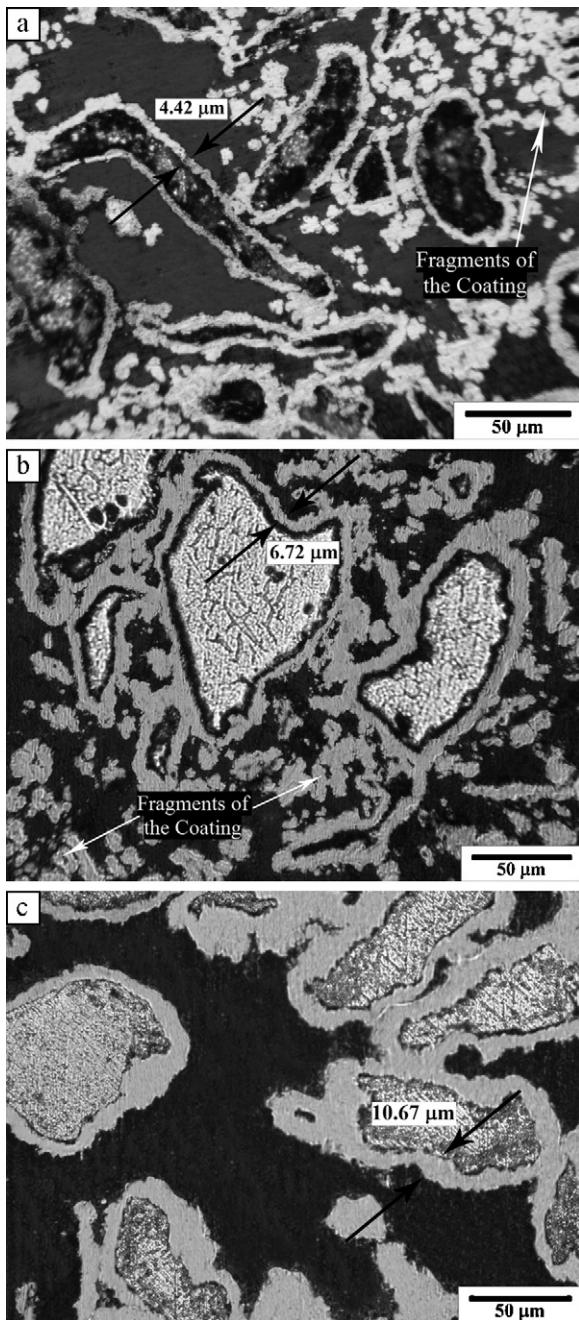
Fig. 4. Typical cross section images of electroless coated magnesium particles at pH values of (a) 5, (b) 6 and (c) 7.

Fig. 5. SEM images of electroless coated powder at pH values of (a) 5, (b) 6 and (c) 7.

Table 1
Average thicknesses of Ni–P coatings at different bath pH values.

Bath pH	Average thickness of the coating (μm)
5	4.65
6	6.47
7	10.14

Table 2
Average thicknesses of Ni–P coatings at different bath temperatures.

Bath temperature (°C)	Average thickness of the coating (μm)
75	–
80	10.14
85	10.95

2. Experimental procedure

In the current study, first the effects of bath pH and temperature on the electroless Ni–P plating on magnesium powder were studied and the suitable values of these parameters were selected. Then by provision of a homogeneous suspension of CNTs in the electroless bath, effect of CNT content in the bath on uniform co-deposition of CNTs into the electroless coating was examined and the best mag-

Table 3
Average thicknesses of Ni–P–CNT coatings at different Mg powder/CNT weight ratios.

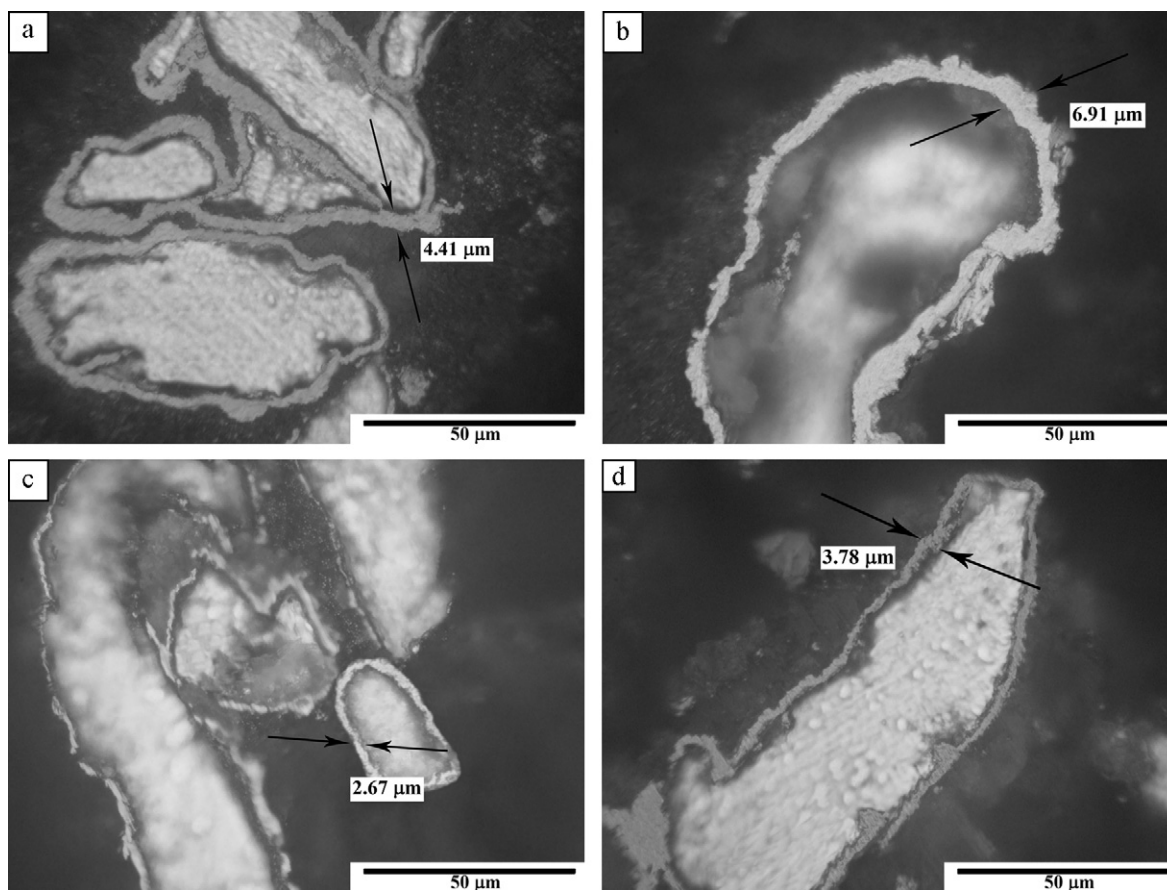| Mg powder/CNT ratio	Average thickness of the coating (μm)
1	4.28
2.5	6.61
4	2.51
6	3.34

Fig. 6. Optical micrographs of composite coatings on magnesium particles at magnesium powder/CNT weight ratios of (a) 1, (b) 2.5, (c) 4 and (d) 6.

nesium powder/CNT ratio for least CNT agglomeration and most reinforcement incorporation was found.

Multi-walled carbon nanotubes with 95% purity were supplied by Research Institute of Petroleum Industry (RIPI, Tehran, Iran). XRD pattern of CNTs and SEM image of CNT agglomerates are shown in Fig. 1. Mo_2C impurity as indicated by the XRD pattern is the major impurity resulted from the CNT fabrication process.

Before each test, CNTs were first purified by immersion in concentrated nitric acid for 20 h at room temperature to remove impurities and then washed with distilled water several times. Ultrasonic agitation was used to disperse CNTs before entering into the bath.

Commercially pure magnesium powder with mean diameter of 150 μm was used as the coating surface. XRD pattern of magnesium powder, showing only magnesium peaks and no significant impurity, and SEM image of the powder are shown in Fig. 2. Magnesium was selected because of its low density and high specific mechanical properties as well as its low ductility [9,20,21]. Simultaneous enhancement in strength and ductility [21] and improved formability [9] has been reported for magnesium–CNT composites.

For direct electroless nickel plating on magnesium, fluoride activation pretreatment and electroless plating from a fluoride containing bath is required [22–27]. Fluoride activation is required for removing the oxide layer from magnesium surface and to create a thin protective film of magnesium fluoride (MgF_2) [27]. It has been mentioned that over-corrosion of magnesium in the electroless bath which is a result of its high activation, can be stopped by replacement of the oxide layer with this protective film [28]. Moreover, it has been indicated that, this protective film can resist only in fluoride solutions [28] and also the presence of fluoride ions in the bath will improve adhesion of the coating [22]. So existence of HF in electroless bath for coating on magnesium is necessary [22–27]. After fluoride activation, magnesium particles were filtered, washed with distilled water and then entered into the bath along with CNTs.

For electroless plating, bath 18071 and Electroless Nickel SLOTONIP 70A process [29] from Schloetter Galvanotechnik were used. Different stages of electroless plating on magnesium powder used in this study are shown in Fig. 3. In each test, 2.5 g of magnesium powder was coated in a glass beaker containing 500 ml of the electroless bath. The Electroless Nickel SLOTONIP 70A process needs some replenishment which mainly depends on the surface throughput [29]. 2.5 ml Nickel Solution SLOTONIP 72 and 2.5 ml Replenisher Solution SLOTONIP 73A is required per dm^2 surface

and per 10 min exposition time [29]. Considering magnesium particles as spheroids with mean diameter of 150 μm, 2.5 g of this powder would have 5.75 dm^2 surface area (almost 20 times more than a sheet of similar weight and 1 mm thickness). So, for each minute of reaction, about 1.5 ml of Nickel Solution SLOTONIP 72 and 1.5 ml of Replenisher Solution SLOTONIP 73A should be added to the bath.

Surface morphology of the composite coating was evaluated using scanning electron microscopy (SEM, Philips XL Series XL30). For each sample a statistically representative number of particles were studied and representative SEM micrographs were selected to show the dominant morphology of the products. Microstructural analyses of the composite coatings were performed by X-ray diffraction (XRD, Philips X'Pert PW 3719) and were characterized by PANalytical X'Pert HighScore software. Moreover, the presence of CNTs in the coatings was proved by energy dispersive X-ray spectroscopy (EDS, Seron AIS-2100). Coating thickness was measured by Image Tool software on optical microscopic images. For each experiment, about 100 particles were selected randomly and thicknesses of different parts of the coatings were measured.

3. Results and discussion

3.1. Effects of bath pH on Ni–P electroless coating of magnesium powder

Effects of bath pH on characteristics of Ni–P electroless coating at bath temperature of 80 °C were studied. Considering typical pH used for electroless plating on magnesium, thickness and morphology of Ni–P coatings on particles were examined at different pH of 5, 6 and 7.

Cross sections of particles coated at different pH values are shown in Fig. 4. Since the electroless bath with pH of 5 is very corrosive for magnesium, the powder looks dark and not shiny in Fig. 4(a). Moreover, the coating is not very uniform and parts of it are separated resulting in considerable coating fragments in the final
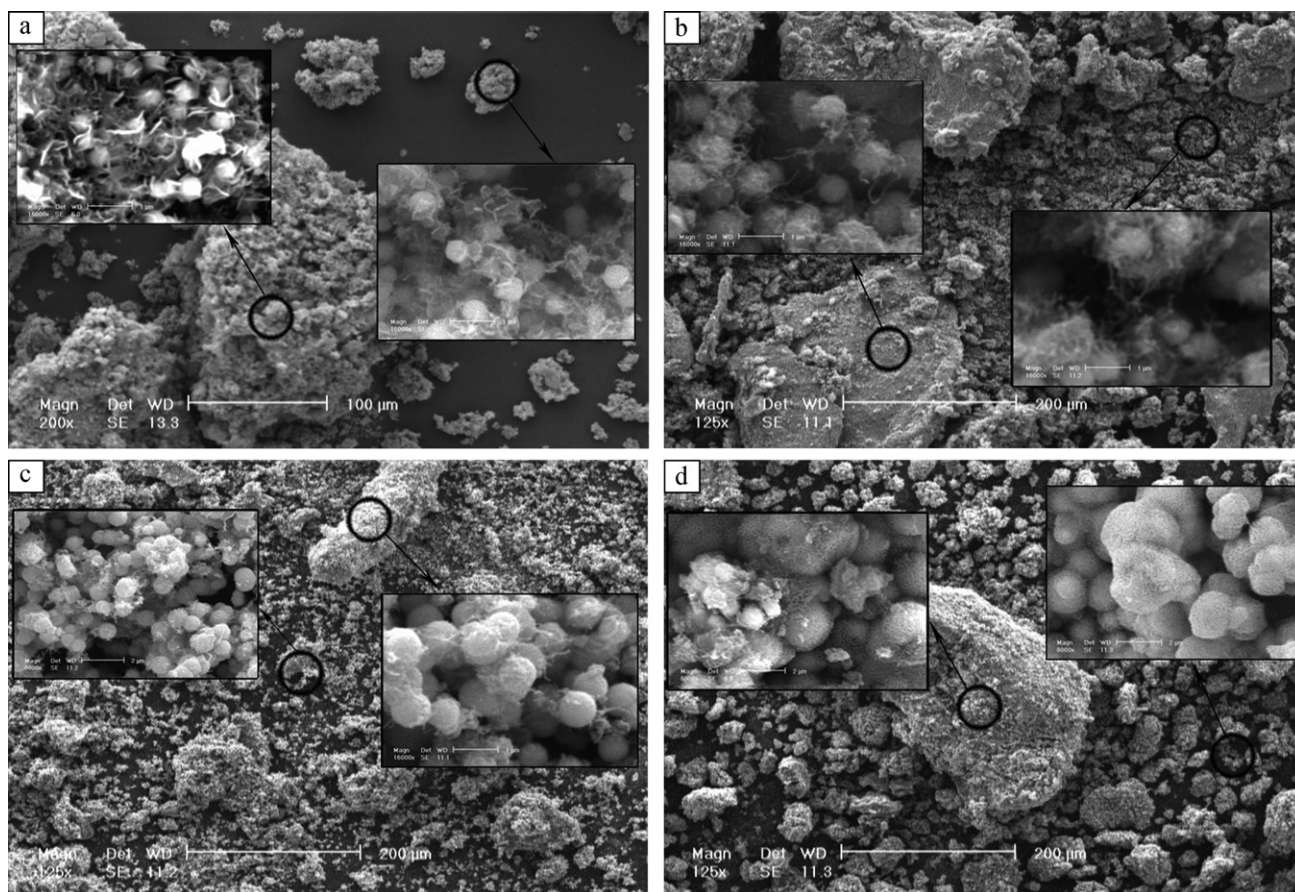
Fig. 7. SEM micrographs of composite coating on magnesium particles at magnesium powder/CNT weight ratios of (a) 1, (b) 2.5, (c) 4 and (d) 6.

product. On the other hand, at pH of 6 (Fig. 4(b)), particles are shiny but the separation of the coating from the surface is still evident and there are some coating fragments in the collected powder as well. At pH of 7, as Fig. 4(c) illustrates, a good adhesion between the coating and the particle surfaces and practically negligible fragmented parts has been achieved.

SEM inlay images of the collected particles in Fig. 5 also indicate the same results. During coating process, individual powder is subjected to a lot of impacts from all the moving particles around which may take off the coating if its adhesion to the substrate is weak.

Adhesion of the coating can be qualitatively assessed by considering the amount of the coating fragments in the SEM images. It is seen that at higher pH, adhesion is improved and pH of 7 gives the best result from this point of view.

Table 1 shows the mean thickness of the coating at different bath pH values. Since the least amount of coating is taken off at pH 7, the highest thickness is achieved at this condition.

Due to the least separation, the apparently strong bonding and the highest coating thickness achieved, pH of 7 was chosen as suitable for Ni–P electroless plating on magnesium powder between the experimental conditions tested.

3.2. Effects of bath temperature on Ni–P electroless coating of magnesium powder

Employing the suitable pH of 7 obtained from the previous section, effect of bath temperature on coating thickness on magnesium particles were studied at bath temperatures of 75, 80 and 85 °C (± 2 °C).

No significant coating reaction was observed at temperatures below about 78 °C. At higher temperatures, however, it started with

a very intense reaction for the first 5 min. Table 2 represents the mean thickness of the coating at different temperatures.

Since electroless plating reactions speed up by temperature, thickest coating was expected at 85 °C. However, as the nickel content of bath was the same for all the experiments, just a slight difference was observed between the bath temperature of 80 and 85 °C. Since control of the reaction is difficult at higher temperature, a temperature between 80 and 85 °C (about 83 °C) was selected as suitable for Ni–P electroless plating on magnesium powder.

3.3. Ni–P–CNT electroless coating of magnesium powder

By adjusting pH and temperature of the electroless bath to 7 and 83 °C, respectively, and simultaneous introduction of magnesium particles and CNTs to the electroless bath, the possibility of co-deposition of CNTs into the coating was examined.

The main objective of the previous tests was to find a suitable processing window for electroless plating on magnesium powder so that a sufficiently high but controllable rate of plating is achieved. This would result in coating that grows with sufficient rate to tangle the CNTs, or in other word, in co-deposition of CNTs into the Ni–P coating.

To study the effect of CNT content on the composite coatings, different weight ratios of magnesium powder/CNT of 1, 2.5, 4 and 6 were tested. Fig. 6 shows that in all of these conditions, uniform coating on magnesium particles was produced. It can be seen that the coatings follow the geometry of the substrates reasonably well. The mean thickness of the coating at different magnesium powder/CNT ratios is presented in Table 3. It appears that some parts of the coatings have been separated from the particles and acted as new surfaces for independent Ni–P coating. These appear as small
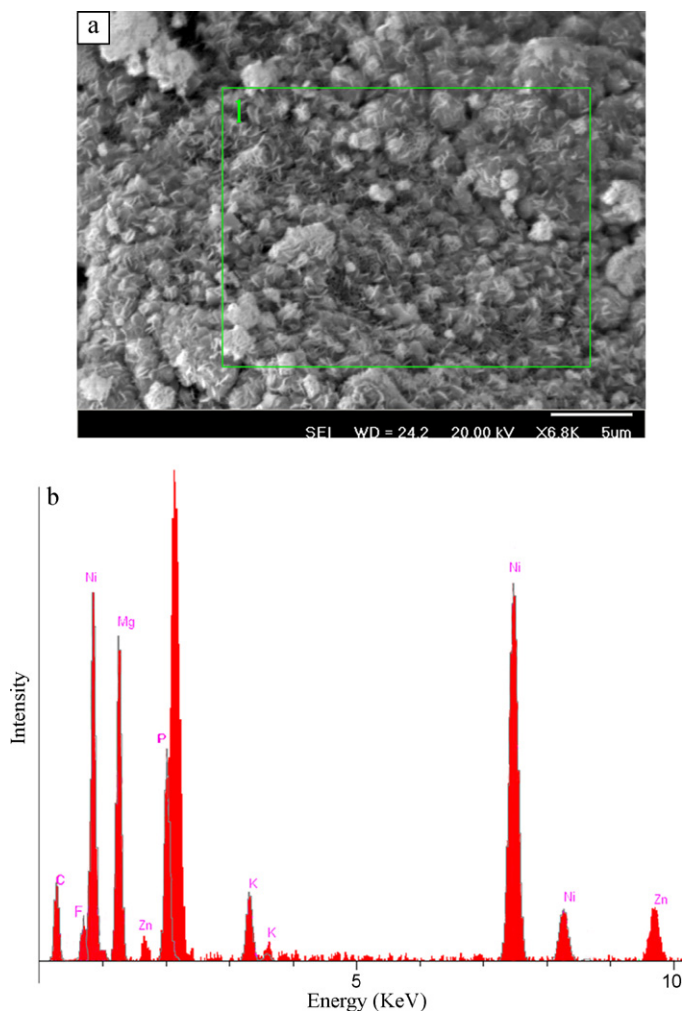
Fig. 8. EDS analysis of composite coating at magnesium powder/CNT weight ratio of 2.5, (a) EDS analysis area and (b) EDS analysis curve.

Fig. 9. XRD patterns of magnesium powder with composite coatings at magnesium powder/CNT weight ratios of (a) 1, (b) 2.5, (c) 4 and (d) 6.

shiny fragments in all micrographs of Fig. 6. This may be due to the difference in the thermal expansion of CNTs and the Ni–P matrix during temperature fluctuations in the bath. Therefore, the mean thicknesses of the composite coatings are less than those without reinforcement produced at the same condition. The thickest coating of 6.61 μm was obtained at ratio of 2.5.

Close SEM observation of the coating features (Fig. 7) illustrates that two types of composite coatings have been produced. The main one is on the magnesium particles where Ni–P electroless coating has been able to entrap the CNTs, and the second type refers to the composite coating fragments which had been previously separated from magnesium particles surfaces and become independent surfaces for deposition of the composite coating.

By reducing the amount of CNT (increasing the weight ratios of magnesium powder/CNT, Fig. 7(a)–(d)), entanglement of CNTs in the composite coatings has diminished. Fig. 7(a), representing the bath containing the highest CNT content, shows a high proportion of CNTs in the composite coating on particles as well as on the separated composite coating fragments. It seems that CNT aggregates did not break thoroughly at this ratio. On the other hand, for the ratio of 2.5 (Fig. 7(b)), although uniform dispersion of CNTs is evident in both types of composite coatings, no sign of CNT aggregates is further evident. Composite coating in Fig. 7(c) (ratio of 4), does not contain as much reinforcement as in the previous samples, whereas at the ratio of 6 (the least amount of CNTs added to
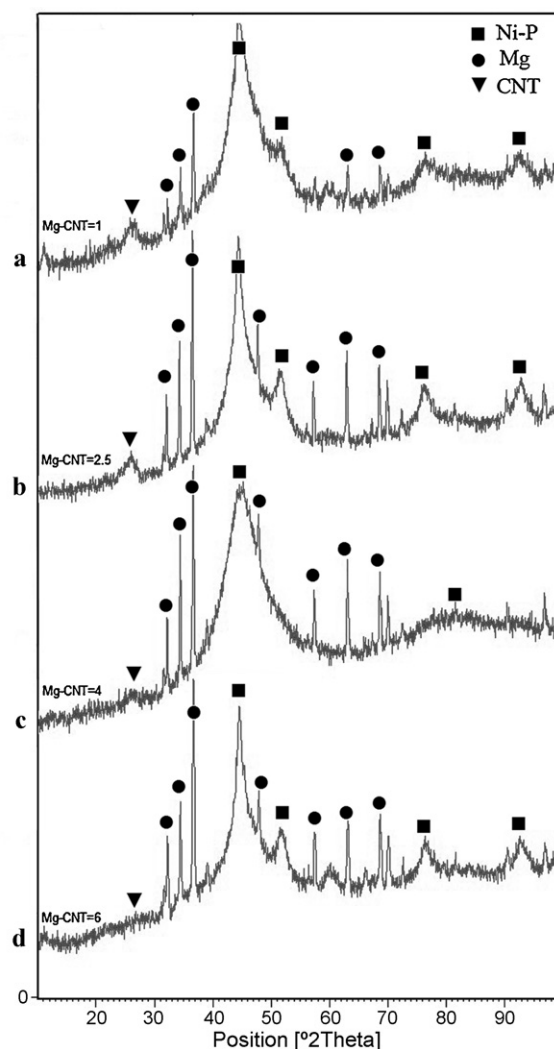
the bath, Fig. 7(d)), no remarkable trace of CNTs in the composite coatings is observed.

Considering the desire for breaking the CNT agglomerates and their uniform dispersion in the composite coating, as well as the need for increased incorporation of CNTs in the composite coatings, magnesium powder/CNT weight ratio of 2.5 was selected as the optimum CNT concentration for electroless composite coating of Ni–P–CNT on magnesium powder. It is believed that the CNT agglomeration problem has been overcome to a great extent because of the intense electroless coating reactions occurring at the employed electroless conditions and the continuous impact from the moving magnesium particles acting as coating surfaces.

The presence of CNTs in the composite coating was further validated by EDS analysis (Fig. 8) which indicated the presence of carbon in the coatings. It must be noted that the highest peak in Fig. 8(b) relates to the gold coating of the specimen.

The presence of CNTs in the coatings can also be shown by XRD analysis. As it is shown in Fig. 1(a), a characteristic peak was observed in XRD pattern of CNTs at 2θ of about 26°. Similar peaks are observed in XRD patterns of magnesium powder with composite coatings (Fig. 9). The intensity of the peak depends on the CNT content of the coating. As Fig. 9 shows, the most intense peak at 2θ of about 26° has occurred for the sample with the highest CNT content (pattern (a)). Evidently this intensity has leveled down by

decreasing the amount of CNTs in the samples. The sharp peaks in the patterns define magnesium, while wide and smooth peaks represent amorphous Ni–P coating.

The results of this study proved that co-deposition of individual disagglomerated CNTs into electroless Ni–P coating is possible under suitable conditions. The fact that the coating surface is provided from moving particles is believed to improve the dispersion of CNTs in the bath. The significant electroless reaction resulted from the large specific surface area of the powder would also help CNTs dispersion considerably.

A major challenge for production of bulk nano-composites is uniform distribution of the highly surface active particles in the matrix and avoiding their agglomeration. The manufactured powder could be used as the feedstock for production of bulk magnesium nano-composites through casting or powder metallurgy routes. The next step in this research is to introduce these Mg–Ni–P–CNT composite particles to molten AZ91 magnesium alloy as the reinforcement instead of pure CNTs. The Ni–P coating around CNTs is expected to improve the wettability of CNTs by the molten metal and results in better CNT/matrix bonding. Also gradual melting of the composite magnesium particles in the melt and gradual release of CNTs into the melt is expected to greatly improve the distribution of the CNTs in the matrix alloy.

4. Conclusions

Electroless Ni–P and Ni–P–CNT plating on magnesium powder was investigated in this work. The suitable pH of the electroless bath was selected as 7 where the best adhesion of the coating to the substrate, the least amount of coating separation and the thickest Ni–P coating on magnesium particles were achieved. No reaction could be spotted at bath temperatures below 78 °C, whereas at higher temperatures the reaction started vigorously and intensified as the temperature increased up to 85 °C. Higher bath temperatures resulted in deposition of a slightly thicker coating. Electroless coatings of Ni–P–CNT were also produced on magnesium powder at different magnesium powder/CNT weight ratios. It was concluded that at sufficiently high growth rates, the Ni–P coatings could entangle CNTs which were well dispersed in the electroless bath. Complete breaking up of CNT agglomerates did not happen at magnesium powder/CNT weight ratio of 1 due to the high CNT content of the coating. On the other hand, at high magnesium powder/CNT ratios of 4 and 6, the amount of entrapped CNTs in the coatings did not seem to be sufficient for the purpose of using the

product as reinforcement in production of bulk magnesium nano-composites. Magnesium powder/CNT weight ratio of 2.5 was found as the most suitable ratio where an acceptable amount and a relatively uniform dispersion of entrapped CNTs were observed in the coating. The presence of CNTs in the composite coating was further confirmed by XRD and EDS analyses.

References

[1] Z. Yang, H. Xu, Y.L. Shi, M.K. Li, Y. Huang, H.L. Li, Mater. Res. Bull. 40 (2005) 1001–1009.
[2] L.Y. Wang, J.P. Tu, W.X. Chen, Y.C. Wang, X.K. Liu, C. Olk, D.H. Cheng, X.B. Zhang, Wear 254 (2003) 1289–1293.
[3] Z. Yang, H. Xu, M.K. Li, Y.L. Shi, Y. Huang, H.L. Li, Thin Solid Films 466 (2004) 86–91.
[4] W.X. Chen, J.P. Tu, Z.D. Xu, W.L. Chen, X.B. Zhang, D.H. Cheng, Mater. Lett. 57 (2003) 1256–1260.
[5] C.S. Chen, X.H. Chen, Z. Yang, W.H. Li, L.S. Xu, B. Yi, Diamond Relat. Mater. 15 (2006) 151–156.
[6] W.X. Chen, J.P. Tu, H.Y. Gan, Z.D. Xu, Q.G. Wang, J.Y. Lee, Z.L. Liu, X.B. Zhang, Surf. Coat. Technol. 160 (2002) 68–73.
[7] Z.H. Li, X.Q. Wang, M. Wang, F.F. Wang, H.L. Ge, Tribol. Int. 39 (2006) 953–957.
[8] A. Esawi, K. Morsi, Composites: Part A 38 (2007) 646–650.
[9] C.S. Goh, J. Wei, L.C. Lee, M. Gupta, Compos. Sci. Technol. 68 (2008) 1432–1439.
[10] Q. Li, A. Viereckl, C.A. Rottmair, R.F. Singer, Compos. Sci. Technol. 69 (2009) 1193–1199.
[11] K. Kondoh, H. Fukuda, J. Umeda, H. Imai, B. Fugetsu, M. Endo, Mater. Sci. Eng. A 527 (2010) 4103–4108.
[12] J. Rams, A. Urena, M.D. Escalera, M. Sanchez, Composites: Part A 38 (2007) 566–575.
[13] E. Carreño-Morelli, J. Yang, E. Couteau, K. Hernadi, J.W. Seo, C. Bonjour, L. Forró, R. Schaller, Met. Powder Rep. 59 (2004) 40–43.
[14] Y.T. Wu, L. Lei, B. Shen, W.B. Hu, Surf. Coat. Technol. 201 (2006) 441–445.
[15] M. Sarret, C. Muller, A. Amell, Surf. Coat. Technol. 201 (2006) 389–395.
[16] G. Jiaqiang, L. Lei, W. Yating, S. Bin, H. Wenbin, Surf. Coat. Technol. 200 (2006) 5836–5842.
[17] D. Dong, X.H. Chen, W.T. Xiao, G.B. Yang, P.Y. Zhang, Appl. Surf. Sci. 225 (2009) 7051–7055.
[18] G.O. Mallory, J.B. Hajdu (Eds.), Electroless Plating Fundamental and Applications, American Electroplaters and Surface Finishers Society (1990).
[19] B. Abbasipour, B. Niroumand, S.M. Monir Vaghefi, Trans. Nonferrous Met. Soc. China 20 (2010) 1561–1566.
[20] Y. Shimizu, S. Miki, T. Soga, I. Itoh, H. Todoroki, T. Hosono, K. Sakaki, T. Hayashi, Y.A. Kim, M. Endo, S. Morimoto, A. Koide, Scr. Mater. 58 (2008) 267–270.
[21] C.S. Goh, J. Wei, L.C. Lee, M. Gupta, Mater. Sci. Eng. A 423 (2006) 153–156.
[22] R. Ambat, W. Zhou, Surf. Coat. Technol. 179 (2004) 124–134.
[23] C. Gu, J. Lian, G. Li, L. Niu, Z. Jiang, J. Alloys Compd. 391 (2005) 104–109.
[24] J. Li, Y. Tian, Z. Huang, X. Zhang, Appl. Surf. Sci. 252 (2006) 2839–2846.
[25] Z. Liu, W. Gao, Surf. Coat. Technol. 200 (2006) 3553–3560.
[26] J. Li, Z. Shao, X. Zhang, Y. Tian, Surf. Coat. Technol. 200 (2006) 3010–3015.
[27] J.E. Gray, B. Luan, J. Alloys Compd. 336 (2002) 88–113.
[28] L.L. Shreir, Magnesium and magnesium alloys, in: Corrosion. Metal/Environment Reactions, vol. 1, second ed., Butterworths, 1979.
[29] 18071 Electroless Nickel SLOTONIP 70A.pdf, www.schloetter.de/en/processes/18-electroless-nickel/ (last visited on 26.06.2010).